Dual-Function Radar-Communications: Information Embedding Using Sidelobe Control and Waveform Diversity

Aboulnasr Hassanien, *Member, IEEE*, Moeness G. Amin, *Fellow, IEEE*, Yimin D. Zhang, *Senior Member, IEEE*, and Fauzia Ahmad, *Senior Member, IEEE*

***Abstract*—We develop a new technique for a dual-function system with joint radar and communication platforms. Sidelobe control of the transmit beamforming in tandem with waveform diversity enables communication links using the same pulse radar spectrum. Multiple simultaneously transmitted orthogonal waveforms are used for embedding a sequence of L_B bits during each radar pulse. Two weight vectors are designed to achieve two transmit spatial power distribution patterns, which have the same main radar beam, but differ in sidelobe levels towards the intended communication receivers. The receiver interpretation of the bit is based on its radiated beam. The proposed technique allows information delivery to single or multiple communication directions outside the mainlobe of the radar. It is shown that the communication process is inherently secure against intercept from directions other than the pre-assigned communication directions. The employed waveform diversity scheme supports a multiple-input multiple-output radar operation mode. The performance of the proposed technique is investigated in terms of the bit error rate.**

***Index Terms*—Bit error rate, dual-function radar-communications, information embedding, sidelobe control, waveform diversity.**

I. Introduction

MOTIVATED by the desire to lower the installation and hardware costs, and driven by the need for radio frequency (RF) spectrum exploitation, the sharing of system platforms and common frequency bands between radar and communications have become the main objectives guiding active sensing and wireless technologies. The co-existence of radar and wireless communication systems can ease competition over bandwidth [1], [2]. It can also complement the functionality of cognitive radio [3] and cognitive radar [4] in enhancing spectrum usage and efficiency. In other words, co-existence of the two platforms within the same frequency band can proceed in concert with the continual search and utilization of the available spectrum [2], [5]–[9]. Sharing of spectrum resources and occupation of the same frequency bandwidth, however, require devising effective approaches to limit cross-interference between the two system functions and to properly apply the spatio-temporal degrees of freedom made possible by advances in waveform design and ubiquitous use of multi-sensor transmit/receive configurations.

Spectrum sharing and the use of common transmit platform between radar and communications require the operator to define the primary and secondary system functions, as demanded by power allocations and preference in beam directivity. The problem of embedding communication symbols into the radar backscatter was addressed in [10], [11]. Incorporating communications as secondary to the primary radar function has been reported in a number of papers [12]–[14]. The embedding of a communication signal into the radar emission was reported in [13].

More recently, a method for information embedding using time modulated arrays has been reported in [14]. The phases of the transmit array elements are adjusted from pulse to pulse in order to introduce variations in the sidelobe levels (SLLs) towards the intended communication receiver. During each radar pulse, the communication receiver detects the SLL and interprets the associated information symbol. Although the waveform does not change from pulse to pulse, it is difficult to design multiple transmit power distribution patterns with the same mainlobe using time modulated arrays. This difficulty is attributed to the fact that the optimization criterion involved in the design is highly nonlinear and computationally demanding.

In this paper, we introduce a new approach to dual-function radar communications (DFRC) using waveform diversity in tandem with sidelobe control. Multiple orthogonal waveforms are used to embed a sequence of L_B bits of information. The sidelobes towards the communication directions are controlled to have two distinct levels. This is achieved by designing two transmit beamforming weight vectors. All waveforms are transmitted simultaneously with one bit embedded in each waveform. The receiver interprets the bit associated with a certain waveform as 0 or 1 based on whether that waveform is radiated

Manuscript received March 27, 2015; revised July 07, 2015 and October 15, 2015; accepted November 21, 2015. Date of publication December 04, 2015; date of current version March 10, 2016. The associate editor coordinating the review of this manuscript and approving it for publication was Dr. Joseph Guerci. This work was supported in part by the National Science Foundation, grant no. AST-1547420. Part of the results reported in this paper has been presented at the IEEE International Radar Conference, Arlington, VA, USA, May 2015.

A. Hassanien, M. G. Amin, and F. Ahmad are with the Center for Advanced Communications, College of Engineering, Villanova University, Villanova, PA 19085 USA (e-mail: hassanien@ieee.org; moeness.amin@villanova.edu; fauzia.ahmad@villanova.edu).

Y. D. Zhang is with the Department of Electrical and Computer Engineering, College of Engineering, Temple University, Philadelphia, PA 19122 USA (e-mail: ydzhang@temple.edu).

Color versions of one or more of the figures in this paper are available online at http://ieeexplore.ieee.org.

Digital Object Identifier 10.1109/TSP.2015.2505667

over the transmit beam associated with the first or the second transmit weight vector, respectively. Note that most modern pulsed radar systems support pulse repetition frequencies in the kHz range [15]–[17] and, therefore, by embedding few bits per pulse, an overall data rate in the range of kbits per sec can be achieved. When the number of transmit array elements is large, higher values of L_B can be used leading to higher data rates. In addition to the waveform diversity, incorporating other types of diversity, e.g., polarization, offers the potential for achieveing even higher data rates.

The proposed technique has the following attributes: (i) The communication message can be delivered to single or multiple communication directions as long as they are located outside the mainlobe where the primary radar function of the system takes place; (ii) The communication process is inherently secure against intercepts from directions other than the pre-assigned communication directions; (iii) The decoding of each bit at the receiver is independent from other neighboring bits in the sequence; (iv) The same set of waveforms are transmitted within every radar pulse which enables the radar to perform coherent processing; (v) The waveform diversity enables the radar to operate in a multiple-input multiple-output (MIMO) mode; and (vi) The communication directions can be adjusted adaptively if the receiver is mounted on a moving platform. The superiority of the proposed approach over the recently developed method in [14] is validated using simulation examples.

The paper is organized as follows. The signal model is described in Section II. Formulations for transmit beamforming designs to achieve quiescent mainlobe response and variable SLLs towards certain directions are presented in Section III. In Section IV, we introduce two novel signaling strategies for the proposed information embedding approach. Performance analysis of the proposed signaling strategies is provided in Section V. Supporting simulation results are presented in Section VI and conclusions are drawn in Section VII.

II. Signal Model

In this section, we develop a DFRC signal model employing waveform diversity and sidelobe control. The proposed system and the one reported in [14] are special cases of the developed model, as will become apparent in the following sections.

Consider a DRFC system equipped with one dual-function transmit array, one radar receive array, and one (or more) communication receive array(s). The transmit and radar receive arrays consist of M_T transmit and M_R receive antennas, respectively, arranged in an arbitrary linear shape. Without loss of generality, we assume that both the radar transmit and receive arrays are closely spaced to each other such that a target located in the far-field would be at the same spatial angle with respect to both arrays. The purpose of the dual-function transmit array is to embed information toward the direction(s) of the communication receiver(s) as a secondary task without affecting the main task of the DFRC system, i.e., the radar operation. The transmit array is used to focus the transmit power within the main beam where the radar operation takes place. The $M_T \times 1$ vector of the baseband representation of the signals at the input of the transmit antennas is given by

$$\mathbf{s}(t;\tau) = \sum_{k=1}^{K} \lambda_k(\tau)\mathbf{u}_k^* \psi_k(t), \tag{1}$$

where t and τ denote the fast-time index (i.e., time within the radar pulse) and the slow-time index (i.e., pulse number), respectively, $\psi_k(t), k = 1, \ldots, K$ are K orthogonal waveforms, $\mathbf{u}_k, k = 1, \ldots, K$ are the $M_T \times 1$ transmit beamforming weight vectors, $\lambda_k(\tau), k = 1, \ldots, K$ are the weights used to determine how much power is assigned to each transmit waveform such that the total transmit power is fixed, and $(\cdot)^*$ denotes the complex conjugate. The waveforms $\psi_k(t), k = 1, \ldots, K$ are assumed to satisfy the orthogonality condition at zero time-delay, that is $\int_{\mathrm{T}} \psi_k(t)\psi_{k'}^*(t) = 0, k \neq k'$, where T is the pulse width. The orthogonal waveforms are used for matched-filtering at the receiver enabling the extraction of the received signals components associated with each transmitted waveform. It is worth noting that the baseband signals in the transmit signal vector $\mathbf{s}(t;\tau)$ need not be orthogonal. The purpose of the transmit weight vectors $\mathbf{u}_k, k = 1, \ldots, K$, is twofold: (i) To focus the transmit power within the main beam of the radar operation while minimizing the power radiated in the out-of-sector area; (ii) To enable information-embedding towards communication directions via achieving certain pre-determined SLLs. Appropriate ways to design the transmit weight vectors will be discussed later in Section III.

Assuming that L far-field targets are located in a certain range-bin within the radar main beam, the $M_R \times 1$ vector of baseband signals received by the radar is expressed as

$$\mathbf{x}(t;\tau) = \sum_{m=1}^{L} \beta_m(\tau) \left(\mathbf{a}^T(\theta_m)\mathbf{s}(t;\tau)\right) \mathbf{b}(\theta_m) + \check{\mathbf{x}}(t;\tau) + \mathbf{z}(t;\tau), \tag{2}$$

where $\beta_m(\tau)$ is the reflection coefficient of the mth target which obeys the Swerling II target model, i.e., the reflectivity remains constant during the entire radar pulse but changes from pulse to pulse, $\mathbf{a}(\theta_m)$ and $\mathbf{b}(\theta_m)$ are the $M_T \times 1$ and the $M_R \times 1$ steering vectors in direction θ_m of the transmit and receive arrays, respectively, $\check{\mathbf{x}}(t;\tau)$ is the $M_R \times 1$ vector comprises the signals that impinge on the receive array from the sidelobe region, $\mathbf{z}(t;\tau)$ is the $M_R \times 1$ vector of additive white Gaussian noise with zero mean and covariance $\sigma_z^2 \mathbf{I}_{M_R}$, $(\cdot)^T$ denotes matrix transpose, and $\mathbf{I}_{M_R}$ is the $M_R \times M_R$ identity matrix. It is worth noting that the processing of the radar received data can be performed directly on the $M_R \times 1$ data vector $\mathbf{x}(t;\tau)$, i.e., without making use of the waveform diversity. Alternatively, incorporating a preprocessing step via matched-filtering the received data to the orthogonal transmitted waveforms may lead to improved radar operation, depending on the transmit signaling strategies used to embed information, as will be discussed later in Section IV. Note that the utilization of the waveform diversity at the radar receiver requires that the transmit waveforms be orthogonal at all time-delays and Doppler-shifts within the range and velocity specifications of the radar. However, in practice, perfectly orthogonal waveforms with overlapped spectral contents cannot be achieved and, therefore, waveforms with low

cross-correlations should be used. The problem of waveform design with low cross-correlations has been extensively studied in the literature (see [18]–[21], and references therein).

Consider J communication receivers located at arbitrary directions within the sidelobe region. The orthogonal waveform dictionary used at the transmitter is assumed to be known to each communication receiver. Assume that the jth communication receiver is equipped with N_j receive antennas arranged in an arbitrary linear shape. The $N_j \times 1$ vector of baseband signals at the output of the receive elements is given as

$$\mathbf{y}_j(t;\tau) = \alpha_j \mathbf{c}_j(\phi_j)\left(\mathbf{a}^T(\theta_j)\mathbf{s}(t;\tau)\right) + \mathbf{n}_j(t;\tau) \tag{3}$$

where α_j is the channel coefficient which summarizes the propagation environment between the transmit array and the jth communication receiver, ϕ_j is the direction-of-arrival (DOA) with respect to the broad side of the jth communication receive array, $\mathbf{c}_j(\phi_j)$ is the steering vector of the receive array in direction ϕ_j, and $\mathbf{n}_j(t;\tau)$ is the $N_j \times 1$ vector of additive white Gaussian noise with zero mean and covariance $\sigma_j^2\mathbf{I}_{N_j}$.

III. Transmit Beamforming Design

In this section, we introduce computationally efficient methods for appropriately designing the $M_T \times 1$ transmit beamforming weight vectors needed for implementing the proposed DFRC methods given in Section IV as well as the method in [14]. The proposed methods require the use of only two transmit beamforming weight vectors while the method in [14] requires the use of $K = 2^{L_B}$ weight vectors. The formulations described in this section design each transmit beamforming weight vector separately and, therefore, enable design of an arbitrary number K of transmit beamforming weight vectors. From the radar operation view point, one key requirement is to maintain a constant transmit power radiation pattern within the main beam of the radar during the entire dwell time, i.e., during the coherent processing interval. On the other hand, in order to embed information in the beamformer, the SLL in the communication directions should be permitted to assume different values. These two key requirements are achieved via appropriate transmit beamforming design. We consider the transmit beamforming design for the following two cases.

Case 1: Narrow Main Beam

Consider the case where the main beam of the radar is focused towards the spatial angle θ_t. A meaningful way to design each transmit weight vector $\mathbf{u}_k, k = 1,\ldots,K$, is to minimize the power radiation level in the out of sector region $\bar{\boldsymbol{\Theta}}$, while maintaining a distortionless response towards the desired direction θ_t. In addition, a certain pre-specified SSL is enforced in the directions where the communication receivers are located. Assuming that the number of communication receivers is less than the number of transmit antennas, i.e., $J < M_T$, the transmit beamforming design can be formulated as the following optimization problem

$$\min_{\mathbf{u}_k} \max_{\theta} \left|\mathbf{u}_k^H \mathbf{a}(\theta)\right|, \quad \theta \in \bar{\boldsymbol{\Theta}}, \tag{4}$$

$$\text{subject to} \mathbf{u}_k^H \mathbf{a}(\theta_t) = 1, \tag{5}$$

$$\mathbf{u}_k^H \mathbf{a}(\theta_j) = \Delta_k, \quad j = 1,\ldots,J, \tag{6}$$

where Δ_k is a pre-determined positive number used to determine the amount of transmit power radiated towards the communications directions over the kth transmit beam and $(\cdot)^H$ denotes the Hermitian operation. The optimization problem (4)–(6) is convex and can be efficiently solved using the interior point methods [22]. It is worth noting that the aforementioned optimization problem should be solved K times, i.e., it should be solved for every $\mathbf{u}_k, k = 1,\ldots,K$. Note that the total number of equality constraints in (5), (6) equals $J+1 \leq M_T$, which is less than or equal to the number of degrees of freedom and, therefore, a feasible solution to (4)–(6) is guaranteed. However, if the number of communication directions is larger than M_T, it is possible that the problem becomes infeasible. In such a case, the equality sign in (6) should be relaxed (e.g., changed to an inequality) and the value of Δ_k should be carefully chosen to warrant a feasible solution to the relaxed formulations of the problem.

Case 2: Wide Main Beam

For the more general case when the radar operation takes place in a wider spatial sector $\boldsymbol{\Theta} = [\theta_{\min}\theta_{\max}]$, one way to design the transmit beamforming weight vectors is to minimize the difference between a desired transmit power radiation pattern and the actual one under the constraints that the sidelobes be bounded by certain pre-defined levels. This can be formulated as the following optimization problem

$$\min_{\mathbf{u}_k} \max_{\theta} \left||G_{\mathrm{d}}(\theta)| - \left|\mathbf{u}_k^H \mathbf{a}(\theta)\right|\right|, \quad \theta \in \boldsymbol{\Theta} \tag{7}$$

$$\text{subject to} \left|\mathbf{u}_k^H \mathbf{a}(\theta)\right| \leq \varepsilon, \quad \theta \in \bar{\boldsymbol{\Theta}}, \tag{8}$$

$$\mathbf{u}_k^H \mathbf{a}(\theta_j) = \Delta_k, \quad j = 1,\ldots,J, \tag{9}$$

where $G_{\mathrm{d}}(\theta)$ is the desired transmit beampattern and ε is a positive number of user's choice used for controlling the SLLs.

In (7)–(9), the objective function fits the actual transmit pattern associated with each transmit beam which is mandated by the radar operation. The set of constraints in (8) is used to upper-bound the transmit power leakage within the sidelobe areas, which is also mandated by the radar operation. Note that the upper bound determined by the parameter ε is the same for all transmit beams. The set of constraints in (9) is associated with the secondary function of the system, which is to embed information by enforcing different SLLs towards the communication directions. It is worth noting that the parameter Δ_k which determines the SLL is different for each transmit beam. Since ε is the highest sidelobe level as mandated by the main radar operation of the system, the condition $\Delta_k \leq \varepsilon, k = 1,\ldots,K$ should be satisfied. However, a tradeoff between the primary radar and the secondary communication operations can be achieved by allowing the SLLs towards the communication directions to be higher than the rest of the sidelobe region. This means that more transmit power is assigned to the communication operation at the price of a decreased transmit gain within the main radar beam. In this case, the set of constraints in (8) should cover the sidelobe region excluding the communication directions.

The optimization problem (7)–(9) is difficult to solve due to the non-convex objective function. Therefore, we reformulate the problem by slightly modifying the objective function. We

set the desired radiation pattern as $G_{\mathrm{d}}(\theta) = e^{\jmath\varphi(\theta)}$, yielding the following optimization problem

$$\min_{\mathbf{u}_k} \max_{\theta_i} \left| e^{\jmath\varphi(\theta_i)} - \mathbf{u}_k^H \mathbf{a}(\theta_i) \right|, \theta_i \in \boldsymbol{\Theta}, i = 1, \ldots, I \quad (10)$$

$$\text{subject to } \left| \mathbf{u}_k^H \mathbf{a}(\theta_p) \right| \leq \varepsilon, \quad \theta_p \in \bar{\boldsymbol{\Theta}}, p = 1, \ldots, P, \quad (11)$$

$$\mathbf{u}_k^H \mathbf{a}(\theta_j) = \Delta_k, \quad j = 1, \ldots, J, \quad (12)$$

where $\theta_i, i = 1, \ldots, I$, and $\theta_p, p = 1, \ldots, P$, are discrete grids of angles used to approximate $\boldsymbol{\Theta}$ and $\bar{\boldsymbol{\Theta}}$, respectively, and $\varphi(\theta)$ is a phase profile of user's choice. The optimization problem (10)–(12) is convex and can be solved in a computationally efficient manner [22]. However, the parameter ε should be carefully chosen to warrant a feasible solution. One way to do this is to solve the following auxiliary problem

$$\min_{\mathbf{u}_k, \varepsilon} \varepsilon \quad (13)$$

$$\text{subject to } \left| \mathbf{u}_k^H \mathbf{a}(\theta_p) \right| \leq \varepsilon, \quad \theta_p \in \bar{\boldsymbol{\Theta}}, p = 1, \ldots, P, \quad (14)$$

$$\mathbf{u}_k^H \mathbf{a}(\theta_j) = \Delta_k, \quad j = 1, \ldots, J, \quad (15)$$

which is guaranteed to have a feasible solution. Denote the solution to (13)–(15) as $\varepsilon_{\min}$. Then, the range of ε values which warrants a feasible solution to the optimization problem (10)–(12) is given as $\varepsilon \geq \varepsilon_{\min}$. Note that the transmit beamforming weight vector obtained by solving (10)–(12) yields a unit magnitude within the main radar beam. However, in practice, the transmit weight vector can be scaled up to the desired transmit gain as long as the total transmit power budget does not exceed the maximum allowed power of the actual system. Further note that scaling up the transmit weight vector results in magnifying the transmit power distribution at all angles equally, i.e., the relative SLLs with respect to the mainlobe remain unchanged.

IV. Signaling Strategies for Information-Embedding

During each radar pulse, the transmitter is assumed to embed L_B bits of information denoted as the binary sequence $B_l, l = 1, \ldots, L_B$. In this section, we propose two signaling strategies for information-embedding using waveform diversity in tandem with sidelobe control. Both signaling strategies require the use of only two transmit beamforming weight vectors denoted as $\mathbf{u}_{\mathrm{H}}$ and $\mathbf{u}_{\mathrm{L}}$. Both $\mathbf{u}_{\mathrm{H}}$ and $\mathbf{u}_{\mathrm{L}}$ are assumed to have the same transmit power radiation pattern except in the spatial directions of the communication receivers where the SLL associated with $\mathbf{u}_{\mathrm{H}}$ is assumed to be higher than the SLL associated with $\mathbf{u}_{\mathrm{L}}$. Either of the optimization problems (4)–(6) or (10)–(12) can be used for designing the aforementioned two weight vectors by choosing $\Delta_k = \Delta_{\mathrm{H}}$ while designing $\mathbf{u}_{\mathrm{H}}$ and $\Delta_k = \Delta_{\mathrm{L}}$ for designing $\mathbf{u}_{\mathrm{L}}$, where $\Delta_{\mathrm{H}} > \Delta_{\mathrm{L}}$. Therefore, the constraints in (6) (similarly (12)) should be restated as $\mathbf{u}_{\mathrm{H}}^H \mathbf{a}(\theta_j) = \Delta_{\mathrm{H}}$ and $\mathbf{u}_{\mathrm{L}}^H \mathbf{a}(\theta_j) = \Delta_{\mathrm{L}}$ while designing $\mathbf{u}_{\mathrm{H}}$ and $\mathbf{u}_{\mathrm{L}}$, respectively. We assume that both $\mathbf{u}_{\mathrm{H}}$ and $\mathbf{u}_{\mathrm{L}}$ are normalized to have unit norm.

A. Proposed Transmit Signaling Strategy 1

The first method requires the use of a number of orthogonal waveforms equals to the number of transmit bits per radar pulse, i.e., L_B waveforms are transmitted simultaneously. During each radar pulse, every transmitted orthogonal waveform is used to deliver one information bit to the communication receivers. The lth orthogonal waveform $\psi_l(t), l = 1, \ldots, L_B$, is radiated either via $\mathbf{u}_{\mathrm{H}}$ for $B_l(\tau) = 0$ or $\mathbf{u}_{\mathrm{L}}$ when $B_l(\tau) = 1$. In this case, the baseband transmit signals in (1) can be rewritten as

$$\mathbf{s}(t;\tau) = \sqrt{\frac{M_T}{L_B}} \sum_{l=1}^{L_B} \left(B_l(\tau) \mathbf{u}_{\mathrm{L}}^* + (1 - B_l(\tau)) \mathbf{u}_{\mathrm{H}}^* \right) \psi_l(t), \quad (16)$$

where the power normalization factor $\sqrt{M_T/L_B}$ is used to ensure that the total transmit power is fixed to M_T.

For the jth communication receiver, the baseband representation of the $N_j \times 1$ signal vector at the output of the receive array is given by

$$\begin{aligned} \mathbf{y}_j(t;\tau) &= \sqrt{\frac{M_T}{L_B}} \alpha_j \mathbf{c}_j(\phi_j) \sum_{l=1}^{L_B} \big(B_l(\tau) \mathbf{u}_{\mathrm{L}}^H \mathbf{a}(\theta_j) \\ &\quad + (1 - B_l(\tau)) \mathbf{u}_{\mathrm{H}}^H \mathbf{a}(\theta_j) \big) \psi_l(t) + \mathbf{n}_j(t;\tau) \\ &= \sqrt{\frac{M_T}{L_B}} \alpha_j \mathbf{c}_j(\phi_j) \sum_{l=1}^{L_B} \left(B_l(\tau) \Delta_{\mathrm{L}} \right. \\ &\quad \left. + (1 - B_l(\tau)) \Delta_{\mathrm{H}} \right) \psi_l(t) + \mathbf{n}_j(t;\tau). \end{aligned} \quad (17)$$

Matched-filtering the received data in (7) to each of the transmitted orthogonal waveforms yields the $N_j \times 1$ data vectors $\mathbf{y}_{j,l}, l = 1, \ldots, L_B$, defined as

$$\mathbf{y}_{j,l}(\tau) = \begin{cases} \sqrt{\frac{M_T}{L_B}} \alpha_j \Delta_{\mathrm{H}} \mathbf{c}(\phi_j) + \mathbf{n}_{j,l}(\tau), & B_l(\tau) = 0, \\ \sqrt{\frac{M_T}{L_B}} \alpha_j \Delta_{\mathrm{L}} \mathbf{c}(\phi_j) + \mathbf{n}_{j,l}(\tau), & B_l(\tau) = 1, \end{cases} \quad (18)$$

where $\mathbf{n}_{j,l}(\tau)$ is the $N_j \times 1$ additive noise vector at the output of the lth matched-filter with the same statistics as that of $\mathbf{n}_j(t;\tau)$.

To detect the transmitted bits, we first apply a simple receive beamforming step, that is

$$y_{j,l}(\tau) = \mathbf{c}_j^H(\phi_j) \mathbf{y}_{j,l}(\tau), \quad l = 1, \ldots, L_B. \quad (19)$$

Then, by performing a simple ratio test, we obtain

$$\hat{B}_l(\tau) = \begin{cases} 0, & \text{if } |y_{j,l}(\tau)| \geq T, \\ 1, & \text{if } |y_{j,l}(\tau)| < T, \end{cases} \quad (20)$$

where T is a threshold. Note that for fast-fading channels, it is difficult to determine the optimal value of the threshold. However, the fast-fading channel case is out of the scope of this paper.

At the radar receiver, the $M_R \times 1$ received data model of (2) can be rewritten as

$$\begin{aligned} \mathbf{x}(t;\tau) &= \sqrt{\frac{M_T}{L_B}} \sum_{m=1}^{L} \beta_m(\tau) \mathbf{b}(\theta_m) \sum_{l=1}^{L_B} \big(B_l(\tau) \mathbf{u}_{\mathrm{L}}^H \mathbf{a}(\theta_m) \\ &\quad + (1 - B_l(\tau)) \mathbf{u}_{\mathrm{H}}^H \mathbf{a}(\theta_m) \big) \psi_l(t) + \check{\mathbf{x}}(t;\tau) + \mathbf{z}(t;\tau). \end{aligned} \quad (21)$$

Matched-filtering $\mathbf{x}(t;\tau)$ to the orthogonal transmitted waveforms yields the $M_R \times 1$ virtual data vectors $\mathbf{x}_l, l = 1, \ldots, L_B$, defined as

$$\begin{aligned} \mathbf{x}_l(\tau) &= \sqrt{\frac{M_T}{L_B}} \sum_{m=1}^{L} \beta_m(\tau) \mathbf{b}(\theta_m) \big(B_l(\tau) \mathbf{u}_{\mathrm{L}}^H \mathbf{a}(\theta_m) \\ &\quad + (1 - B_l(\tau)) \mathbf{u}_{\mathrm{H}}^H \mathbf{a}(\theta_m) \big) + \check{\mathbf{x}}_l(\tau) + \mathbf{z}_l(\tau) \end{aligned} \quad (22)$$

where $\check{\mathbf{x}}_l(\tau) \triangleq \int \check{\mathbf{x}}(t;\tau) \psi_l^*(t) dt$ and $\mathbf{z}_l(\tau) \triangleq \int \mathbf{z}(t;\tau) \psi_l^*(t) dt$.

Stacking the virtual data vectors in (22) in one column vector, the $L_B M_R \times 1$ extended data vector is expressed as

$$\tilde{\mathbf{x}}(\tau) = \sqrt{\frac{M_T}{L_B}} \sum_{m=1}^{L} \beta_m(\tau) \tilde{\mathbf{a}}(\theta_m) \otimes \mathbf{b}(\theta_m) + \mathbf{x}_i(\tau) + \tilde{\mathbf{z}}(\tau). \quad (23)$$

where $\tilde{\mathbf{a}}(\theta)$ is the $L_B \times 1$ diversity vector, defined as

$$\tilde{\mathbf{a}}(\theta) \triangleq \begin{bmatrix} B_1(\tau)\mathbf{u}_{\mathrm{L}}^H \mathbf{a}(\theta) + (1 - B_1(\tau))\, \mathbf{u}_{\mathrm{H}}^H \mathbf{a}(\theta) \\ \vdots \\ B_{L_B}(\tau)\mathbf{u}_{\mathrm{L}}^H \mathbf{a}(\theta) + (1 - B_{L_B}(\tau))\, \mathbf{u}_{\mathrm{H}}^H \mathbf{a}(\theta) \end{bmatrix}, \quad (24)$$

$\otimes$ is the Kronecker product, and $\mathbf{x}_i(\tau) \triangleq [\check{\mathbf{x}}_1^T(\tau), \ldots, \check{\mathbf{x}}_{L_B}^T(\tau)]^T$ and $\tilde{\mathbf{z}}(\tau) \triangleq [\mathbf{z}_1^T(\tau), \ldots, \mathbf{z}_{L_B}^T(\tau)]^T$ are the $L_B M_R \times 1$ out of sector interference and additive zero-mean white Gaussian noise with variance σ_z^2, respectively. The virtual data in (23) corresponds to the virtual data model used in MIMO radar. When performing DOA estimation, the use of the data in (23) leads to better angular estimation accuracy and angular resolution than that of the single-input-multiple-output (SIMO) configuration adopted in [14]. For detailed discussions on the advantages of MIMO radar over SIMO radar in terms of DOA estimation performance, see [23]–[31]. We note that the use of (23) for DOA estimation requires the bit sequence $B_l(\tau), l = 1, \ldots, L_B$ to be known at the radar receiver, thus making it suitable for monostatic radar applications. In case the bit sequence is not available at the radar receiver (e.g., in bistatic radar applications), the data in (21) can be used for DOA estimation and localization.

B. Proposed Transmit Signaling Strategy 2

This signaling strategy utilizes $2L_B$ orthogonal waveforms to deliver an L_B bits message sequence during a single radar pulse. More specifically, two orthogonal waveforms are dedicated to delivering one bit. In this case, the baseband transmit signals in (1) can be rewritten as

$$\mathbf{s}(t;\tau) = \sqrt{\frac{M_T}{2L_B}} \sum_{l=1}^{L_B} \left(\left(B_l(\tau)\mathbf{u}_{\mathrm{L}}^* + (1 - B_l(\tau))\, \mathbf{u}_{\mathrm{H}}^*\right) \psi_l(t) + \left(B_l(\tau)\mathbf{u}_{\mathrm{H}}^* + (1 - B_l(\tau))\, \mathbf{u}_{\mathrm{L}}^*\right) \psi_{L_B+l}(t) \right). \quad (25)$$

Here, $2L_B$ waveforms are transmitted simulaneously and, as such, a normalization factor of $\sqrt{M_T/2L_B}$ is used to ensure that the total transmit power is fixed to M_T.

At the jth communication receiver, the baseband representation of the $N_j \times 1$ signal vector at the output of the receive array is given by

$$\begin{aligned} \mathbf{y}_j(t;\tau) &= \sqrt{\frac{M_T}{2L_B}} \alpha_j \mathbf{c}_j(\phi_j) \\ &\quad \cdot \sum_{l=1}^{L_B} \left(\left(B_l(\tau)\mathbf{u}_{\mathrm{L}}^H \mathbf{a}(\theta_j) + (1 - B_l(\tau))\mathbf{u}_{\mathrm{H}}^H \mathbf{a}(\theta_j)\right) \psi_l(t) \right. \\ &\quad \left. + \left(B_l(\tau)\mathbf{u}_{\mathrm{H}}^H \mathbf{a}(\theta_j) + (1 - B_l(\tau))\mathbf{u}_{\mathrm{L}}^H \mathbf{a}(\theta_j)\right) \psi_{L_B+l}(t) \right) \\ &\quad + \mathbf{n}_j(t;\tau) \\ &= \sqrt{\frac{M_T}{2L_B}} \alpha_j \mathbf{c}_j(\phi_j) \sum_{l=1}^{L_B} \left((B_l(\tau)\Delta_{\mathrm{L}} + (1 - B_l(\tau))\Delta_{\mathrm{H}})\, \psi_l(t) \right. \\ &\quad \left. + \left(B_l(\tau)\Delta_{\mathrm{H}} + (1 - B_l(\tau))\, \Delta_{\mathrm{L}}\right) \psi_{L_B+l}(t) \right) \\ &\quad + \mathbf{n}_j(t;\tau). \end{aligned} \quad (26)$$

Matched-filtering the received data in (26) to each of the transmitted orthogonal waveforms yields the $N_j \times 1$ vector pair, $\mathbf{y}_{j,l}$ and $\mathbf{y}_{j,L_B+l}$, $l = 1, \ldots, L_B$, defined as

$$\begin{aligned} \mathbf{y}_{j,l}(\tau) &= \sqrt{\frac{M_T}{2L_B}} \alpha_j \left(B_l(\tau)\Delta_{\mathrm{L}} \right. \\ &\quad \left. + (1 - B_l(\tau))\, \Delta_{\mathrm{H}}\right) \mathbf{c}(\phi_j) + \mathbf{n}_{j,l}(\tau), \end{aligned} \quad (27)$$

$$\begin{aligned} \mathbf{y}_{j,L_B+l}(\tau) &= \sqrt{\frac{M_T}{2L_B}} \alpha_j \left(B_l(\tau)\Delta_{\mathrm{H}} \right. \\ &\quad \left. + (1 - B_l(\tau))\, \Delta_{\mathrm{L}}\right) \mathbf{c}(\phi_j) + \mathbf{n}_{j,L_B+l}(\tau). \end{aligned} \quad (28)$$

Measuring the signal strengths at the receiver as $\eta_l(\tau) = |\mathbf{c}^H(\phi_j)\mathbf{y}_{j,l}(\tau)|$ and $\eta_{L_B+l}(\tau) = |\mathbf{c}^H(\phi_j)\mathbf{y}_{j,L_B+l}(\tau)|$, $l = 1, \ldots, L_B$, the lth transmitted bit can be detected using the test

$$\hat{B}_l(\tau) \begin{cases} 0, & \text{if } \eta_l(\tau) \geq \eta_{L_B+l}(\tau), \\ 1, & \text{if } \eta_l(\tau) < \eta_{L_B+l}(\tau). \end{cases} \quad (29)$$

At the radar receiver, the $M_R \times 1$ received data model of (2) can be rewritten as

$$\begin{aligned} \mathbf{x}(t;\tau) &= \sqrt{\frac{M_T}{2L_B}} \sum_{m=1}^{L} \beta_m(\tau) \mathbf{b}(\theta_m) \\ &\quad \cdot \sum_{l=1}^{L_B} \left(\left(B_l(\tau)\mathbf{u}_{\mathrm{L}}^H \mathbf{a}(\theta_m) + (1 - B_l(\tau))\mathbf{u}_{\mathrm{H}}^H \mathbf{a}(\theta_m)\right) \psi_l(t) \right. \\ &\quad \left. + \left(B_l(\tau)\mathbf{u}_{\mathrm{H}}^H \mathbf{a}(\theta_m) + (1 - B_l(\tau))\mathbf{u}_{\mathrm{L}}^H \mathbf{a}(\theta_m)\right) \psi_{L_B+l}(t) \right) \\ &\quad + \check{\mathbf{x}}(t;\tau) + \mathbf{z}(t;\tau). \end{aligned} \quad (30)$$

Matched-filtering $\mathbf{x}(t;\tau)$ to the orthogonal transmitted waveforms yields L_B pairs of the $M_R \times 1$ virtual data vectors $\{\mathbf{x}_l, \mathbf{x}_{L_B+l}\}, l = 1, \ldots, L_B$, defined as

$$\begin{aligned} \mathbf{x}_l(\tau) &= \sqrt{\frac{M_T}{2L_B}} \sum_{m=1}^{L} \beta_m(\tau) \left(B_l(\tau)\mathbf{u}_{\mathrm{L}}^H \mathbf{a}(\theta_m) \right. \\ &\quad \left. + (1 - B_l(\tau))\, \mathbf{u}_{\mathrm{H}}^H \mathbf{a}(\theta_m)\right) \mathbf{b}(\theta_m) + \check{\mathbf{x}}_l(\tau) + \mathbf{z}_l(\tau), \end{aligned} \quad (31)$$

$$\begin{aligned} \mathbf{x}_{L_B+l}(\tau) &= \sqrt{\frac{M_T}{2L_B}} \sum_{m=1}^{L} \beta_m(\tau) \left(B_l(\tau)\mathbf{u}_{\mathrm{H}}^H \mathbf{a}(\theta_m) \right. \\ &\quad \left. + (1 - B_l(\tau))\, \mathbf{u}_{\mathrm{L}}^H \mathbf{a}(\theta_m)\right) \mathbf{b}(\theta_m) + \check{\mathbf{x}}_{L_B+l}(\tau) + \mathbf{z}_{L_B+l}(\tau). \end{aligned} \quad (32)$$

Stacking the virtual data vectors in (31) and (32) into a tall column vector yields the $2L_B M_R \times 1$ extended data vector $\tilde{\mathbf{x}}(\tau) \triangleq [\mathbf{x}_1^T(\tau), \ldots, \mathbf{x}_{2L_B}^T(\tau)]^T$ which can be used for DOA estimation.

A few comments are in order with regards to the two proposed signaling strategies. Unlike strategy 1, since the detection of a certain bit in strategy 2 is performed by comparing the received signal strength associated with one waveform to that of another waveform, no threshold is required. Moreover, in signaling strategy 2, the number of waveforms transmitted via $\mathbf{u}_H$ equals the number of waveforms transmitted via $\mathbf{u}_L$ regardless of the binary sequence comprising the embedded information. As such, from the radar operation view point, any clutter or interference located in the sidelobe region will result in the same signal reflections during the entire coherent processing interval. On the other hand, the signaling strategy 1 uses the bit sequence

to determine which waveform will be transmitted via a particular SLL. This may cause clutter to slightly change from pulse to pulse during the coherent processing interval. For illustration, assume that the number of 0's in the bit sequence during a certain pulse is L_0 and the number of 1's during the same pulse is L_1, i.e., $L_B = L_0 + L_1$. Signaling strategy 1 results in L_0 waveforms being transmitted via $\mathbf{u}_H$ and the remaining L_1 waveforms being transmitted via $\mathbf{u}_L$. If L_0 and L_1 are not equal, which is likely to be the case, then any clutter or interference located in the communication direction will result in a slightly changing signal reflections. Note that the aforementioned advantages of strategy 2 over strategy 1 are obtained at the expense of using twice the number of orthogonal waveforms as compared to the signal strategy 1.

V. Performance Analysis

In this section, we discuss the performance analysis of the dual-function radar-communications system. We derive the bit error rate (BER) expression which enables the selection of the optimal threshold used at the communications receivers.

A. BER Analysis for Transmit Signaling Strategy 1

For the first method developed in Section IV-A, the receive beamformer output (19), when $B_l(\tau) = 0$ is transmitted, simplifies to

$$\begin{aligned} y_{j,l}(\tau) &= \mathbf{c}^H(\phi_j)\mathbf{y}_{j,l}(\tau) \\ &= \sqrt{\frac{M_T}{L_B}} N_j \alpha_j \Delta_{\mathrm{H}} + \mathbf{c}^H(\phi_j)\mathbf{n}_{j,l}(\tau) \\ &= \tilde{\alpha}_{j,l} + n_{j,l}(\tau), \end{aligned} \tag{33}$$

where $\tilde{\alpha}_{j,l} \triangleq \sqrt{M_T/L_B} N_j \alpha_j \Delta_{\mathrm{H}}$ is a complex variable which is assumed to be constant and $n_{j,l}(\tau)$ is white Gaussian noise with zero-mean and variance $\tilde{\sigma}^2 = N_j \sigma_n^2$. Let $\eta_l \triangleq |y_{j,l}(\tau)|$ be the magnitude of the communication receiver output (33). Since $\tilde{\alpha}_{j,l}$ is constant and $n_{j,l}(\tau)$ is zero-mean Gaussian noise, η_l is a random variable with Rician distribution that follows the probability density function

$$\mathrm{R}(\eta_l | A_{\mathrm{H}}, \tilde{\sigma}) = \frac{\eta_l}{\tilde{\sigma}^2} e^{\frac{-\left(\eta_l^2 + A_{\mathrm{H}}^2\right)}{2\tilde{\sigma}^2}} I_0\left(\frac{\eta_l A_{\mathrm{H}}}{\tilde{\sigma}^2}\right), \tag{34}$$

where $A_{\mathrm{H}} \triangleq |\sqrt{M_T/L_B} N_j \alpha_j \Delta_{\mathrm{H}}|$ and $I_0(\cdot)$ is the modified Bessel function of the first kind with order zero.

Let $P_0 = p(B_l(\tau) = 0)$ be the probability of transmitting 0. Then, the event of wrongly detecting 1 instead of 0 in performing the test (20) occurs when η_l is less than the threshold T. Therefore, the probability of detecting 1 given 0 is transmitted, denoted as $P(1|0)$, is given by,

$$\begin{aligned} P(1|0) &= P(\eta_l < T) \\ &= \int_{\eta_l = 0}^{T} \mathrm{R}(\eta_l | A_{\mathrm{H}}, \tilde{\sigma}) d\eta_l \\ &= 1 - Q\left(\frac{A_{\mathrm{H}}}{\tilde{\sigma}}, \frac{T}{\tilde{\sigma}}\right), \end{aligned} \tag{35}$$

where $Q(\cdot, \cdot)$ is the Marcum Q-function.

On the other hand, when $B_l(\tau) = 1$ is transmitted, the probability density function of the magnitude or the received communications signal η_l is given by the Rician distribution $\mathrm{R}(\eta_l | A_{\mathrm{L}}, \tilde{\sigma})$, where $A_{\mathrm{L}} = |\sqrt{M_T/L_B} N_j \alpha_j \Delta_L|$. In this case, the probability of erroneously detecting 0 while 1 is transmitted is given by

$$P(0|1) = P(\eta_l \geq T) = \int_{\eta_l = T}^{\infty} R(\eta_l | A_{\mathrm{L}}, \tilde{\sigma}) d\eta_l = Q\left(\frac{A_{\mathrm{L}}}{\tilde{\sigma}}, \frac{T}{\tilde{\sigma}}\right). \tag{36}$$

Therefore, the probability of error P_e can be expressed as

$$P_e = P_0 P(1|0) + P_1 P(0|1), \tag{37}$$

where $P_1 = p(B_l(\tau) = 1)$. Since the transmitted waveforms are orthogonal (i.e., independent from each other), the detection of the data bits associated with the individual waveforms is also independent. Therefore, the overall probability of error can be obtained by averaging over the probability of error associated with the individual bits. If the exact value of η_{q} (otherwise, it can be estimated) associated with $B_l(\tau) = 0$ and $B_l(\tau) = 1$ is known at the receiver, then the optimal threshold T can be taken as the value that minimizes the P_e in (37).

B. BER Analysis for Transmit Signaling Strategy 2

For the second proposed method described in Section IV-B, the detection does not involve comparing the magnitude of the received signal to a threshold. Instead, detecting the lth bit $B_l(\tau)$ involves comparing the magnitude of the received signal associated with the lth waveform to the magnitude of the received signal due to the $L_B + l$ th waveform. Let us assume that $B_l(\tau) = 0$ is transmitted. Substituting $B_l(\tau) = 0$ in (27) and (28) yields

$$\mathbf{y}_{j,l}(\tau) = \sqrt{\frac{M_T}{2L_B}} \alpha_j \Delta_{\mathrm{H}} \mathbf{c}(\phi_j) + \mathbf{n}_{j,l}(\tau) \tag{38}$$

$$\mathbf{y}_{j,L_B+l}(\tau) = \sqrt{\frac{M_T}{2L_B}} \alpha_j \Delta_{\mathrm{L}} \mathbf{c}(\phi_j) + \mathbf{n}_{j,L_B+l}(\tau) \tag{39}$$

Therefore, the signal strengths used for detection (c.f., (29)) become

$$\eta_l = \left| \sqrt{\frac{M_T}{2L_B}} N_j \alpha_j \Delta_{\mathrm{H}} + \mathbf{c}(\phi_j)^H \mathbf{n}_{j,l}(\tau) \right| \tag{40}$$

$$\eta_{L_B+l} = \left| \sqrt{\frac{M_T}{2L_B}} N_j \alpha_j \Delta_{\mathrm{L}} + \mathbf{c}^H(\phi_j) \mathbf{n}_{j,L_B+l}(\tau) \right|. \tag{41}$$

The variables η_l and η_{j,L_B+l} follow the Rician probability distributions $\mathrm{R}(\eta_l | \tilde{A}_{\mathrm{H}}, \tilde{\sigma})$ and $\mathrm{R}(\eta_{L_B+l} | \tilde{A}_{\mathrm{L}}, \tilde{\sigma})$, respectively, where $\tilde{A}_{\mathrm{H}} = |\sqrt{M_T/2L_B} N_j \alpha_j \Delta_{\mathrm{H}}|$ and $\tilde{A}_{\mathrm{L}} = |\sqrt{M_T/2L_B} N_j \alpha_j \Delta_{\mathrm{L}}|$. Note that η_l and η_{L_B+l} are independent from each other and, therefore, the joint probability density function equals to the multiplication of the individual probability density functions, that is,

$$\mathrm{R}(\eta_l, \eta_{L_B+l}) = \mathrm{R}(\eta_l | \tilde{A}_{\mathrm{H}}, \tilde{\sigma}) \mathrm{R}(\eta_{L_B+l} | \tilde{A}_{\mathrm{L}}, \tilde{\sigma}) \tag{42}$$

Therefore, the probability of erroneously detecting 1, given 0 is transmitted, can be expressed as

$$\begin{aligned} P(1|0) &= P(\eta_{L_B+l} \geq \eta_l) \\ &= \int_{\eta_l=0}^{\infty} \int_{\eta_{L_B+l}=\eta_l}^{\infty} \mathrm{R}(\eta_l, \eta_{L_B+l}) d\eta_{L_B+l} d\eta_l \\ &= \int_{\eta_l=0}^{\infty} R(\eta_l|\tilde{A}_{\mathrm{H}}, \tilde{\sigma}) \\ &\quad \cdot \left\{ \int_{\eta_{L_B+l}^{\infty}=\eta_l} R(\eta_{L_B+1}|\tilde{A}_{\mathrm{L}}, \tilde{\sigma}) d\eta_{L_B+l} \right\} d\eta_l \\ &= \int_{\eta_l=0}^{\infty} R(\eta_l|\tilde{A}_{\mathrm{H}}, \tilde{\sigma}) Q\left(\frac{\tilde{A}_{\mathrm{L}}}{\tilde{\sigma}}, \frac{\eta_l}{\tilde{\sigma}}\right) d\eta_l, \end{aligned} \tag{43}$$

where $R(\eta_l, \eta_{L_B+l})d\eta_{L_B+l}$ is the two dimensional joint Rician probability density function.

It is worth noting that when $B_l(\tau) = 1$ is transmitted, the same two waveforms are used but interchanged over the two transmit beams, i.e., $\psi_l(t)$ is radiated via $\mathbf{u}_L$ while $\psi_{L_B+l}(t)$ is radiated via $\mathbf{u}_H$. This implies that, at the communication receiver, the roles of η_l and η_{L_B+l} will be interchanged. Therefore, the probability of erroneously detecting 0 while 1 is transmitted will be given by (43) as well, i.e.,

$$P(1|0) = P(0|1). \tag{44}$$

C. BER Analysis for the Method in [14]

We also derive the BER expressions for the DFRC method in [14]. This method maps L_B bits of information into one of 2^{L_B} communications symbols which are represented by one of the 2^{L_B} SLLs during each radar pulse. Different SLLs towards the communications direction can be achieved through designing the transmit beamforming weight vectors $\mathbf{u}_k, k = 1, \ldots, 2^{L_B}$ by solving the optimization problem (10)–(12) while choosing

$$\Delta_k = \Delta_H - \frac{k-1}{2^{L_B}-1}(\Delta_H - \Delta_L), \quad k = 1, \ldots, 2^{L_B}. \tag{45}$$

Note that the SLLS associated with $\mathbf{u}_1$ and $\mathbf{u}_{2^{L_B}}$ are given by Δ_H and Δ_L, respectively while the remaining $2^{L_B}-2$ SLLs are uniformly spaced between Δ_H and Δ_L. The signal transmitted during a certain pulse is given by

$$\mathbf{x}(t;\tau) = \sqrt{M_T}\mathbf{u}\psi(t), \tag{46}$$

where the $M_T \times 1$ vector $\mathbf{u}$ during each radar pulse is taken as one of the aforementioned 2^{L_B} weight vectors depending on the actual bits to be encoded during that pulse, $\sqrt{M_T}$ is a normalization factor used to insure that the total transmit power is normalized to M_T, and $\psi(t)$ is a single transmit waveform which is transmitted during every radar pulse.

The signal at the output of the matched-filter at the communication receiver in this case is given as

$$\mathbf{y}_j(\tau) = \sqrt{M_T}\alpha_j \left(\mathbf{u}^H \mathbf{a}(\theta_j)\right) \mathbf{c}(\phi_j) + \mathbf{n}_j(\tau). \tag{47}$$

Measuring the signal strength at the receiver as $\eta_{\mathrm{SLL}}(\tau) = |\mathbf{c}^H(\phi_j)\mathbf{y}_j(\tau)|$, the transmitted symbol can be detected by comparing η_{SLL} to the set of $2^{L_B}-1$ thresholds $T_k, k = 1, \ldots, 2^{L_B}-1$. Then, the detected symbol can be converted to the corresponding bit sequence. The probability of erroneous detection of the kth symbol is given as

$$\begin{aligned} P_{e,k} &= P(\eta_{\mathrm{SLL}} < T_{k-1}) + P(\eta_{\mathrm{SLL}} \geq T_k) \\ &= 1 - Q\left(\frac{A_{\mathrm{k}}}{\tilde{\sigma}}, \frac{T_k}{\tilde{\sigma}}\right) + Q\left(\frac{A_{\mathrm{k}}}{\tilde{\sigma}}, \frac{T_{k-1}}{\tilde{\sigma}}\right), \end{aligned} \tag{48}$$

where $A_{\mathrm{k}} = |\sqrt{M_T}N_j\alpha_j\Delta_{\mathrm{k}}|$. Note that for $k = 1$ and $k = 2^{L_B}$, T_0 and $T_{2^{L_B}}$ do not exist and, therefore, the first and the second terms in (48) do not exist, respectively. The overall probability of symbol error can be obtained by the statistical average over the individual probability of symbol error (48). In case, all symbols are transmitted with equal probability, the overall probability of symbol error simplifies to the mathematical average over the individual probability of symbol error, i.e., the summation of all probability of symbol error terms divided by the number of symbols.

D. Illustrative Example

For the purpose of comparison, we consider the case of $L_B = 2$, i.e., two bits are required to be embedded within each radar pulse. The method in [14] converts the two bit information into one of four symbols which can be communicated via one of four SLLs. Assuming that the variance of the noise at the communications receiver is unity, Fig. 1 depicts the Rician probability distribution associated with the four different symbols. The variance of the noise is taken as $\tilde{\sigma}_n^2 = 1$. The four sidelobe levels are chosen as $A_1 = 5.6234$, $A_2 = 3.9364$, $A_3 = 2.2494$, and $A_4 = 0.5623$ which corresponds to $10\log(A_1^2/\tilde{\sigma}_n^2) = 15$ dB, $10\log(A_2^2/\tilde{\sigma}_n^2) = 11.9020$ dB, $10\log(A_3^2/\tilde{\sigma}_n^2) = 7.0412$ dB, and $10\log(A_4^2/\tilde{\sigma}_n^2) = -5$ dB, respectively. Note that the values of the SLLs are chosen to be equally separated from each other on linear scale which corresponds to non-uniform spacing on logarithmic scale. The detection thresholds are indicated as vertical dashed lines in the figure. The tails of the different Rician distributions on either side of the thresholds represent the regions where the detection fails leading to erroneous decoding.

Fig. 2 show the Rician probability density functions versus the magnitude of the received signal at the communication receiver for the first proposed signaling strategy. In this case, the high and low SLLs are chose such that $A_H = A_1/\sqrt{2}$ and $A_L = A_4/\sqrt{2}$. The reason for this choice is that the method in [14] assigns the entire transmit power to a single waveform, whereas the first proposed signalizing strategy divides the total transmit power equally among two orthogonal waveforms. Note that the two Rician distribution functions associated with the high and low SLLs are the same for the individual bits because each bit is associated with an independent waveform, i.e., the received signals associated with the individual bits are separable from each other at the receiver. The threshold used to detect the embedded bit is indicated as a vertical line in the figure. Fig. 2 also depicts the tails of the Rician distributions which correspond to detection error.

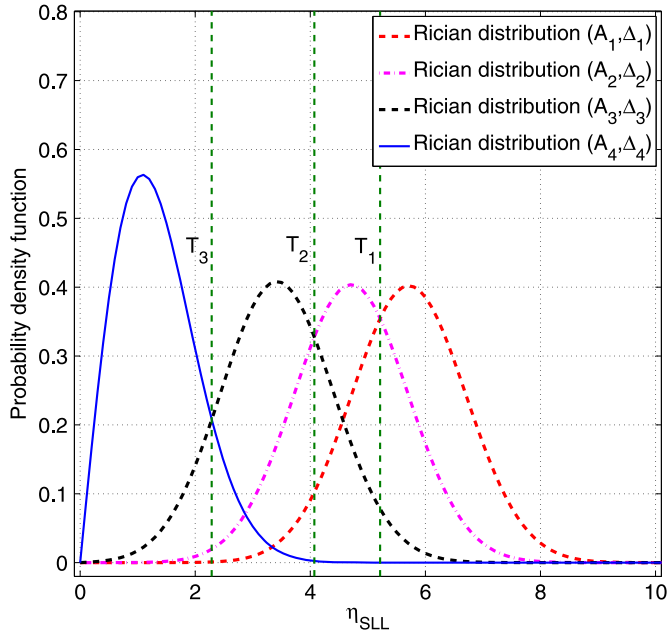

Fig. 1. Rician probability density function versus magnitude of received signal strength; SLLs based method in [14].

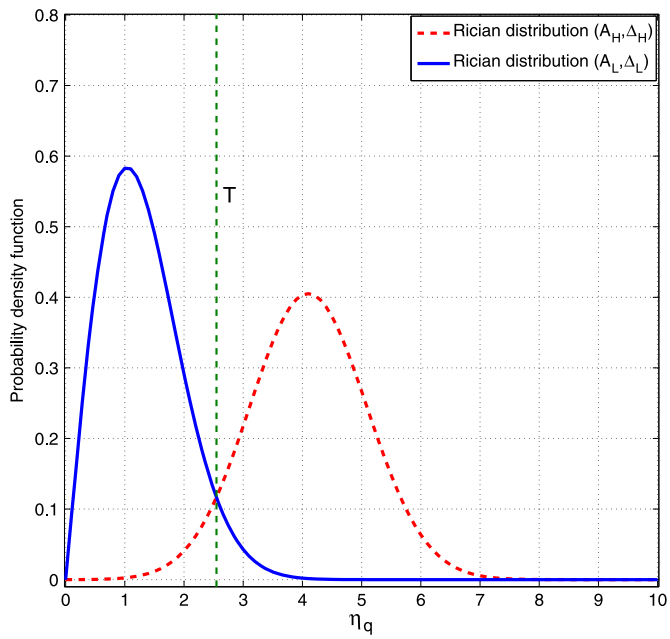

Fig. 2. Rician probability density function versus magnitude of received signal strength; first proposed transmit signaling strategy.

For the second proposed transmit signaling strategy, two pairs of waveforms are used simultaneously; one pair per information bit. Therefore, four waveforms are used to embed two bits per pulse which means one quarter of the total transmit power is assigned to each waveform. Fig. 3 shows the two dimensional Rician distribution function by choosing $\tilde{A}_{\rm H} = A_1/2$ and $\tilde{A}_{\rm L} = A_4/2$, respectively. The detection in this case is performed by comparing the magnitude of the received signal due to one waveform to the magnitude of the received signal due to the second waveform of the pair. This comparison is indicated by the diagonal line in Fig. 3. The right lower triangle of the

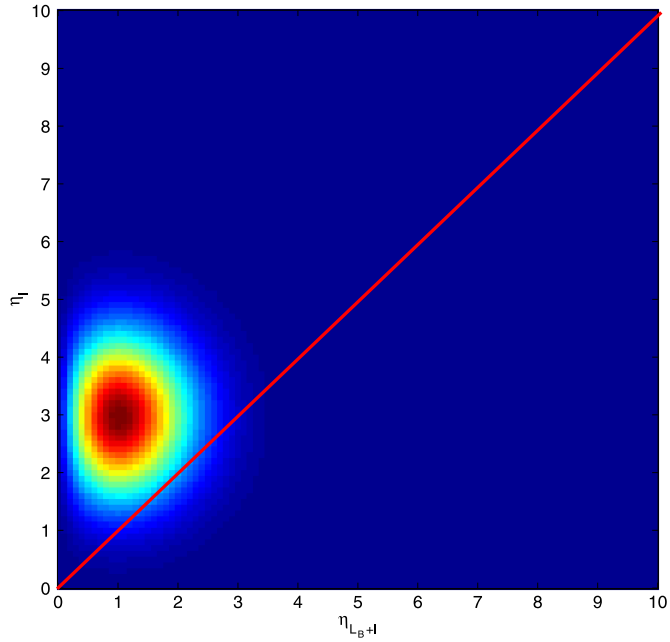

Fig. 3. Two dimensional joint Rician probability density function versus magnitude of received signal strengths associated with a pair of orthogonal waveforms; second proposed transmit signaling strategy.

joint Rician distribution function represent the region of detection error, i.e., the region where the signal associated with the lower SLL is higher than the signal associated with the higher one.

We calculate the theoretical BER for the two proposed methods using the expressions (36), (43). It is worth noting that (48) enables calculating the symbol error rate for the method in [14]. However, the BER can be straightforwardly calculated by considering the probability of erroneous detection of the individual bits, i.e., by integrating the portions of the Rician probability distributions in Fig. 1 which corresponds to a bit error. Fig. 4 shows the BER curves versus $10\log A_1^2/\sigma_n^2$ for all methods considered. We vary all other SLLs in the same rate such that total transmit power used for all methods remain the same, i.e., for example $\tilde{A}_{\rm H} = A_H/\sqrt{2} = A_1/2$ has always been satisfied. It is clear from the figure that the two proposed transmit signaling strategies have theoretically much lower BER as compared to the method in [14]. This fact will be demonstrated by simulation examples in the following section. It is worth noting that the theoretical BER derivations given above correspond to the case of transmission and reception of unencoded data. However, the BER associated with encoded data can be lower than the BER associated with the unencoded one. This will be investigated further in the simulation section.

VI. Simulation Results

We consider a uniform linear transmit array consisting of $M_T = 10$ antennas spaced one-half wavelength apart. In addition to the radar operation within the mainbeam, we assume that, during each radar pulse, a communication message of $L_B = 2$ bits is delivered towards the communication directions located in the sidelobe region. In all simulation examples, we provide a comparison between the two proposed methods and the method

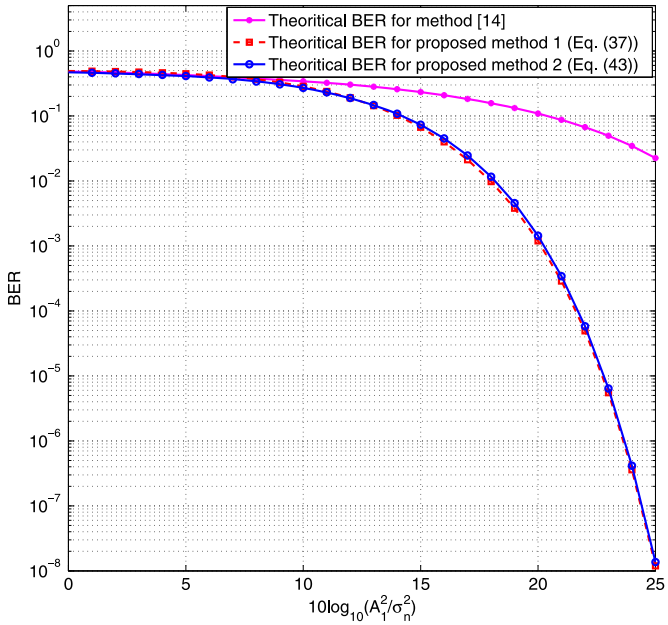

Fig. 4. Theoretical BER versus the SNR associated with the highest SLL.

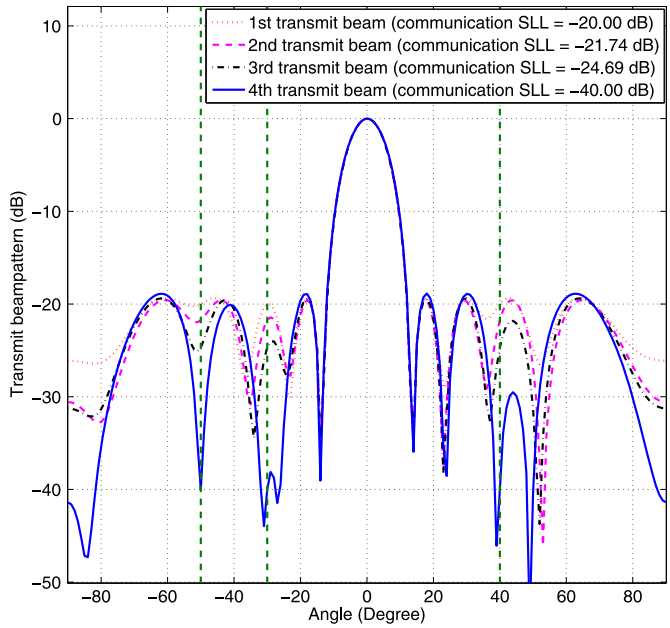

Fig. 5. Transmit power distribution versus spatial angle; Example 1.

of [14]. To implement the SLL based method in [14], we design $2^{L_B} = 4$ transmit beamforming weight vectors. On the other hand, only two transmit weight vectors are used for the proposed methods.

Example 1: Transmit Beampattern Design for Narrow Main Beam

We first investigate the possibility of synthesizing transmit power distribution patterns with a fixed mainbeam towards a specific angle and variable SLLs towards multiple communication directions. This scenario enables delivering a certain communication message simultaneously to multiple communication receivers. Four transmit weight vectors $\mathbf{u}_k, k = 1, \ldots, 4$, which focus their individual mainbeams towards the radar operation direction $\theta_{\text{radar}} = 0^\circ$, are obtained by solving (4)–(6). Three communication receivers are assumed to be located in directions $\theta_1 = -50^\circ$, $\theta_2 = -30^\circ$, and $\theta_3 = 40^\circ$, respectively. The communication SLLs associated with $\mathbf{u}_k, k = 1, \ldots, 4$, are constrained to be at $\Delta_1^2 = 0.01$ or -20 dB, $\Delta_2^2 = 0.0033$ or -21.76 dB, $\Delta_3^2 = 0.0066$ or -24.77 dB, and $\Delta_4^2 = 10^{-4}$ or -40 dB, all relative to the mainbeam. For all other sidelobe directions, the SLLs are controlled by choosing $\varepsilon = 0.1$. Fig. 5 shows the normalized transmit power distribution patterns versus angle for all transmit weight vectors. We observe that, as expected, all transmit weight vectors have almost the same pattern within the mainbeam, which implies that the radar operation will not be affected if the waveform is radiated via either transmit beam. Further, the SLLs towards the communication directions are clearly separated from each other, thereby enabling the communication receivers to detect which transmit SLL was used during a certain radar pulse and, in turn, determine the associated information message. Therefore, information embedding can proceed by choosing a certain waveform to be radiated over either of the transmit beams.

Example 2: BER Performance for Narrow Main Beam

Next, we use the setup in Example 1 to investigate the performance of the two proposed methods in terms of the BER and compare it with the technique in [14]. Note that the latter technique employs a single waveform in tandem with 4 SSLs towards the communication direction to deliver $L_B = 2$ bits of information. On the other hand, we employ two orthogonal waveforms to deliver two bits per pulse, i.e., one waveform per bit, for the first proposed method and four orthogonal waveforms, i.e., two waveforms per bit, for the second proposed method. To test the BER, a sequence of 10^6 symbols unencoded (two bits each) are transmitted. In addition, a convolutional encoder of rate 2/3 is applied to the original sequence resulting in 1.5×10^6 encoded sequence. Both the unencoded and the encoded sequences are embedded independently using the method of [14] and the proposed two methods. The communication receiver is assumed to be equipped with $N = 10$ receive antennas arranged in a non-uniform linear array where the positions of the elements are drawn randomly from the interval [0,4.5], measured in wavelength. The received encoded sequence is decoded using a Viterbi decoder. The BERs versus the signal-to-noise ratio (SNR) for the three methods is shown in Fig. 6 for both the unencoded as well as the encoded data sequences. Clearly, both proposed methods achieve superior BER performance as compared to the method of [14]. Note that the latter method transmits 25% of the information via each of the four beams. Therefore, intersymbol interference becomes a considerable source of detection error resulting in performance degradation. This phenomenon is expected to be worse if longer binary sequences are used. It is worth noting that, for all methods tested, the BER associated with the encoded sequence outperforms the BER associated with the unencoded sequence. However, this BER superiority comes at the price of slower data transmission rate.

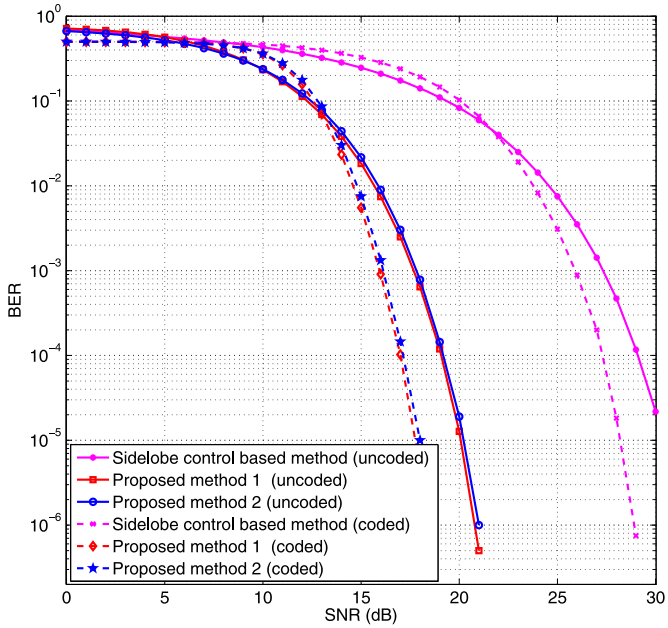

Fig. 6. BER versus SNR; Example 2.

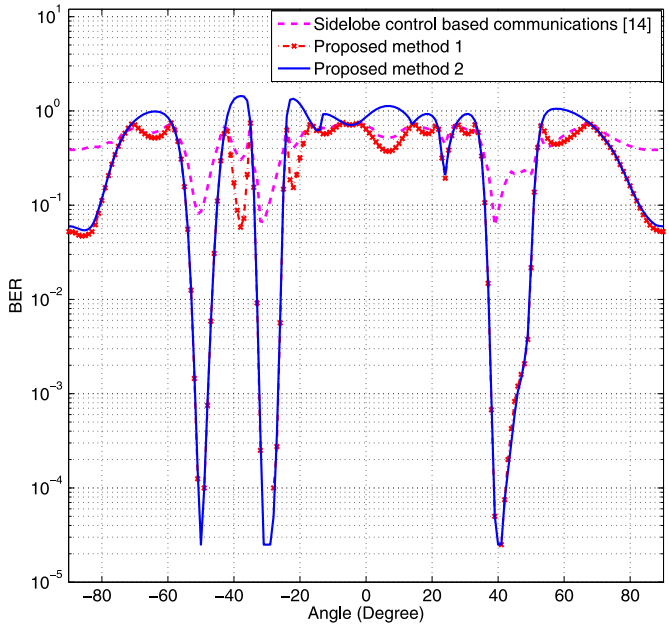

Fig. 7. BER versus angle; Example 3.

Example 3: Probability of Intercept for Narrow Main Beam

In this example, we test the security of the communication process and show that the proposed methods prevent communications interception from directions other than the intended ones. To this end, we calculate the BER versus transmission angle for all methods tested. We use the same set up as in Example 2, except that the SNR is fixed at 10 dB. The BERs are calculated based on transmitting 1.5×10^6 symbols of encoded data sequence. The Viterbi decoder is used to decode the received data. Fig. 7 depicts the BER versus angle for the three considered methods, which shows that the BER assumes high values for directions other than the intended communication directions in all cases. This means that all methods have inherent security against information interception from directions other than the communication directions. It can be also confirmed from the figure that the two proposed methods have a better BER towards the communication directions as compared to the method of [14].

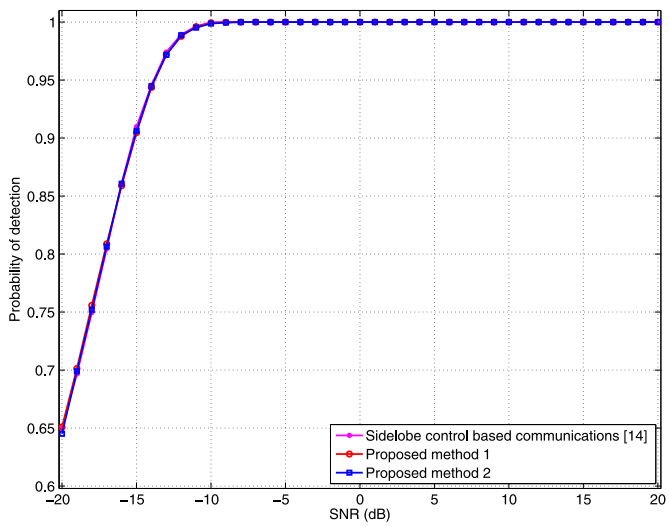

Fig. 8. Probability of target detection versus SNR; Example 4.

Example 4: Probability of Target Detection for Narrow Main Beam

Next, we evaluate the performance of the radar operation within the main beam focused towards $\theta_{\text{radar}} = 0°$, in terms of the probability of target detection. We assume a single target located in the far-field at direction $\theta_t = 0°$. The number of radar receive elements is chosen to be $M_R = 10$, with the antennas arranged in an arbitrary linear array configuration, co-located with the transmit array. The target is considered to be detected if the received power from θ_t exceeds a certain threshold, which is set to unity in this example. Fig. 8 shows the probability of target detection versus SNR. We observe that all methods tested provide similar target detection performance, which implies that the process of information embedding in the sidelobe region does not adversely affect the primary radar operation.

Example 5: Transmit Beampattern Design for Wide Main Beam

In this example, we assume that the main radar operation takes place within the sector $\boldsymbol{\Theta} = [-10°10°]$. We further assume that the radar operation requires the power level emitted in the sidelobe areas to be at least 20 dB lower than the mainlobe. The communication operation remains in the sidelobe region, where a single communication direction of $\theta = -50°$ is considered. Again, we assume that $L_B = 2$ bits of information are to be transmitted during every radar pulse. The four transmit weight vectors are designed by solving (10)–(12). The parameters $\Delta_k, k = 1, \ldots, 4$, and ε are chosen to have the same values as in Example 1. The first and fourth designed vectors are used for the proposed methods, while all four are employed for implementing the SLL based method of [14]. Fig. 9 plots the transmit power distribution patterns for all four transmit weight

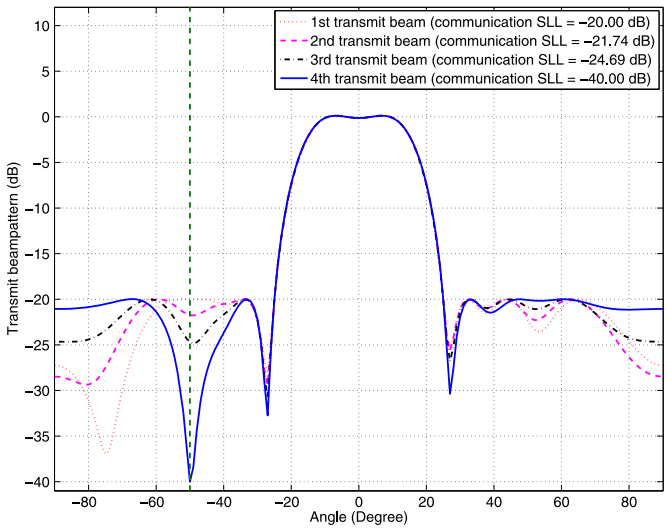

Fig. 9. Transmit power distribution versus spatial angle; Example 5.

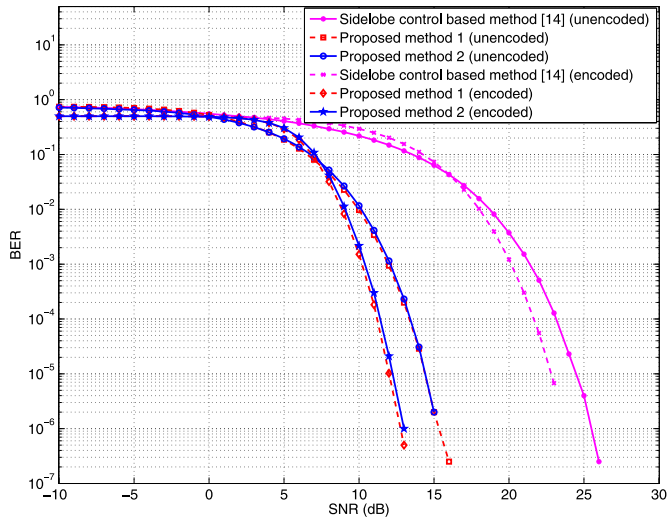

Fig. 10. BER versus SNR; Example 6.

vectors, which clearly shows that all patterns are identical within the sector $\boldsymbol{\Theta}$, whereas the SLLs towards the communication directions are distinct from each other, thereby enabling information embedding. Note that the difference between two adjacent SSLs towards the communication direction is the same in terms of log-scale magnitude.

Example 6: BER Performance for Wide Main Beam

This example tests the BER versus SNR for the communication receiver located at -50° using the transmit beamforming vector designs of Example 5. During each radar pulse, the transmitter embeds 2 bits of information and the communication receiver performs detection on a pulse by pulse basis. Similar to Example 2, the experiment is carried over 10^6 independent trials of unencoded data. The information sequence is generated randomly. Also, a convolutional encoder and a Viterbi decoder are used to perform the simulation using encoded data sequence. Fig. 10 shows the BERs versus SNR for all methods tested. It is clear that the two proposed methods achieve superior BER performance as compared to the method of [14]. The figure also shows that the BER associated with the case of encoded data sequence is better than that for the case of unencoded data for all methods tested. Again, this comes at the price of slower data transmission rate.

Example 7: DOA Estimation Performance for Wide Main Beam

This example evaluates the DOA estimation performance of the radar operation. We assume two targets located in the far-field at angles 3° and 5°, respectively. The target reflection coefficients are assumed to be constant during each radar pulse, but change from pulse to pulse and are drawn from a normal distribution. The number of radar receive array elements is chosen as $M_R = 10$. The number of pulses used is 100, i.e., 100 data snapshots are used at the radar receiver to build the data covariance matrix. The MUSIC algorithm is used to perform DOA estimation for all methods tested. The two targets are assume to be resolved provided

$$|\hat{\theta}_i - \theta_i| \leq \frac{|\theta_2 - \theta_1|}{2}, \quad i = 1, 2, \tag{49}$$

is satisfied [32]. The root-mean square error (RMSE) and the probability of target resolution are averaged over 1000 independent runs. Figs. 11 and 12 show the RMSE versus SNR and the probability of target resolution versus SNR, respectively. It can be observed that the two proposed methods outperform the method of [14]. This is because the method of [14] transmits a single waveform at any given pulse and as such, does not exploit any waveform diversity, i.e., the size of the data at the radar receiver has dimensions $M_R \times 1$. For the first proposed method, assuming that $P(B_l(\tau) = 0) = P(B_l(\tau) = 1) = 0.5$, the transmitter utilizes $\mathbf{u}_H$ alone (i.e., when $B_1(\tau) = 0$ and $B_2 = 0$) during 25% of the time and $\mathbf{u}_L$ alone (i.e., when $B_1(\tau) = 1$ and $B_2 = 1$) during 25% of the time. That is, during half of the time (i.e., when $B_1(\tau) = B_2$), the received data (at the radar receiver) depends on either $\mathbf{u}_H$ or $\mathbf{u}_L$ alone, but not both of them at the same time. During the remaining time (i.e., when $B_1(\tau) \neq B_2$), the received data can be virtually extended into a $2M_R \times 1$ vector, where the first $M_R \times 1$ part of the data is a function of $\mathbf{u}_H$ and the second $M_R \times 1$ data part is a function of $\mathbf{u}_L$, leading to a virtually extended array. This increased dimensionality results in improved DOA estimation performance as compared to the method of [14]. For the second proposed method, two different waveforms are transmitted all the time leading to $2M_R \times 1$ virtual data 100% of the time. This results in even better DOA estimation performance and probability of source resolution as compared to the first method. However, the performance improvement is achieved at the expense of using twice the number of orthogonal waveforms as compared to the first proposed method.

Example 8: Effect of Sidelobe Modulation on Out-of-Sector Interference Localization

The final example tests the effect of varying the SLLs from pulse to pulse on the performance of DOA estimation of powerful sources located in the sidelobe region. Since the sources are located outside the mainbeam of the radar, they are treated as interference. We use the same setup as that of Example 7, except that two interfering sources are assumed to be located at directions -52° and -48°, respectively. The interference reflection

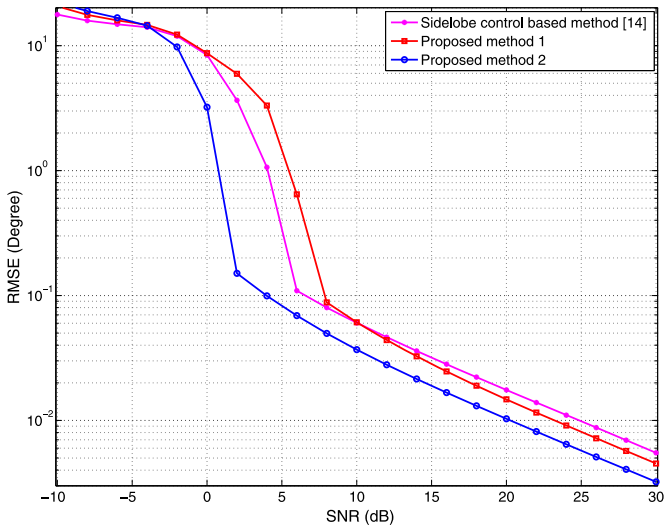

Fig. 11. RMSE versus SNR; Example 7.

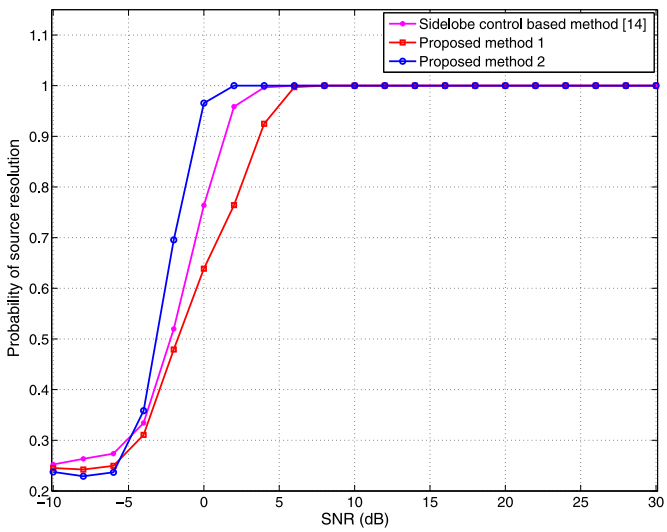

Fig. 12. Probability of target resolution versus SNR; Example 7.

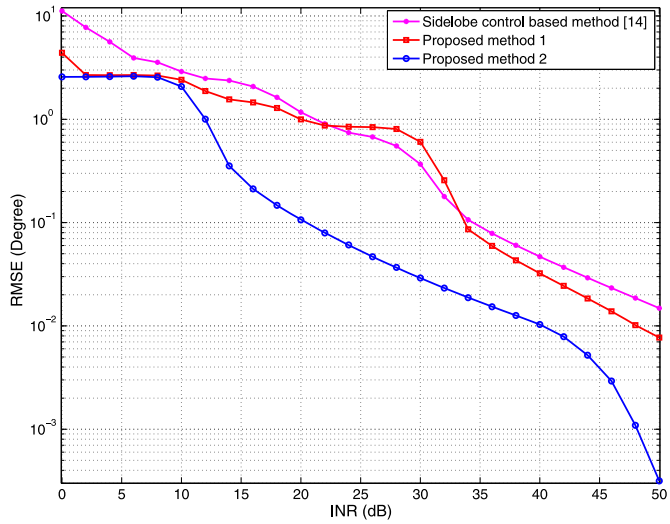

Fig. 13. RMSE versus INR; Example 8.

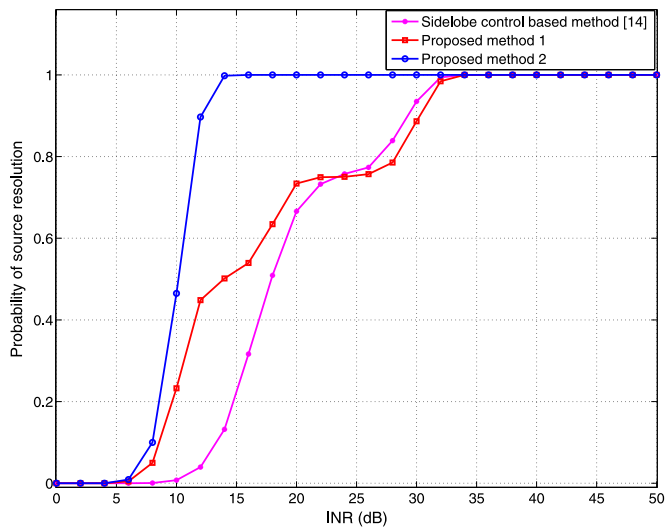

Fig. 14. Probability of interfering source resolution versus INR; Example 8.

coefficients are assumed to be constant during each radar pulse, but change from pulse to pulse and are drawn from a normal distribution. We assume that the secondary function of the system embeds two bits of information during each radar pulse where the probabilities of embedding '0' and embedding '1' are equal. Therefore, the method of [14] utilizes four different sidelobe levels which means that 25% of the received data snapshots have interference strength proportional to each one of the four sidelobe levels. This variation in the interference strength within a CPI is expected to degrade the interference DOA estimation performance. For the first proposed method, the sidelobe variation takes only two distinct levels, namely 'high' and 'low'. This implies that 25% of the received data snapshots exhibit interference strength proportional to the high sidelobe level, 25% of the received data snapshots exhibit interference strength proportional to the low sidelobe level, and the remaining 50% exhibit interference strength proportional to the average of the high and low SLLs. For each embedded bit using the second proposed method, two orthogonal waveforms are emitted simultaneously; one via each of the high and low SLLs. In this case, the strength of the received interference signal is proportional to the average of both the high and low SLLs for all radar pulses.

The RMSE and the probability of source resolution are averaged over 500 independent runs. Figs. 13 and 14 show the RMSE versus interference-to-noise ratio (INR) and the probability of target resolution versus INR, respectively. It can be observed from the two figures that the proposed method 1 slightly outperforms the method of [14] because it exhibits less SLL variation. The figures also show that the proposed method 2 has the best performance because the strength of the received interference signal is not affected by variations in the SLLs during the entire CPI.

VII. Conclusion

A new approach to dual-function radar-communication system was introduced, which recognizes the primary radar function of the system and employs array beam sidelobes to transmit the digital communication signals. Two array responses associated with the same main beam were designed

using two different transmit weight vectors in order to achieve distinct spatial transmit power distribution patterns outside the radar designated beam. This distinction was aimed at creating two sidelobe levels in the direction of the designated communication receiver. The bi-level sidelobes at specific angles were used in conjunction with multiple orthogonal waveforms to enable effective co-existence between the radar and communications platforms. The number of orthogonal waveforms was chosen as equal to the length of the bit sequence to be delivered during each radar pulse. The use of bi-level sidelobe radiation pattern enables a communication receiver to interpret the information bit in each orthogonal waveform. The proposed technique permits information delivery to single or multiple communication directions as long as they are located outside the mainlobe of the radar. The communication process was shown to be inherently secure against intercept from directions other than the pre-assigned communication directions. The effectiveness of the proposed technique and its superiority over existing DFRC techniques in terms of the BER performance were demonstrated through extensive simulations.

REFERENCES

[1] H. Griffiths, S. Blunt, L. Chen, and L. Savy, "Challenge problems in spectrum engineering and waveform diversity," in *Proc. IEEE Radar Conf. (RadarCon 2013)*, Ottawa, ON, Canada, Apr.–May 2013, pp. 1–5.

[2] D. W. Bliss, "Cooperative radar and communications signaling: The estimation and information theory odd couple," in *Proc. IEEE Radar Conf. (RadarCon 2014)*, Cincinnati, OH, USA, May 2014, pp. 50–55.

[3] A. J. Goldsmith and L. J. Greenstein, *Principles of Cognitive Radio*. Cambridge, U.K.: Cambridge Univ. Press, 2012.

[4] S. Haykin, *Cognitive Dynamic Systems: Perception-Action Cycle, Radar and Radio*. Cambridge, U.K.: Cambridge Univ. Press, 2012.

[5] M. Jamil, H. Zepernick, and M. I. Pettersson, "On integrated radar and communication systems using Oppermann sequences," in *Proc. IEEE Military Commun. Conf. (MILCOM 2008)*, Nov. 2008, pp. 1–6.

[6] S. C. Surender, R. M. Narayanan, and C. R. Das, "Performance analysis of communications & radar coexistence in a covert UWB OSA system," in *Proc. IEEE Global Commun. Conf. (GLOBECOM 2010)*, Miami, FL, USA, Dec. 2010, pp. 1–5.

[7] Y. L. Sit, C. Sturm, L. Reichardt, T. Zwick, and W. Wiesbeck, "The OFDM joint radar-communication system: An overview," in *Proc. Int. Conf. Adv. Satellite Space Commun. (SPACOMM 2011)*, 2011, pp. 69–74.

[8] J. R. Guerci, R. M. Guerci, A. Lackpour, and D. Moskowitz, "Joint design and operation of shared spectrum access for radar and communications," in *Proc. IEEE Int. Radar Conf. (RadarCon 2015)*, Arlington, VA, USA, May 2015, pp. 761–766.

[9] A. Hassanien, M. G. Amin, Y. D. Zhang, and F. Ahmad, "A dual function radar-communications system using sidelobe control and waveform diversity," in *Proc. IEEE Int. Radar Conf. (RadarCon 2015)*, Arlington, VA, USA, May 2015, pp. 1260–1263.

[10] S. D. Blunt, P. Yatham, and J. Stiles, "Intrapulse radar-embedded communications," *IEEE Trans. Aerosp. Electron. Syst.*, vol. 46, no. 3, pp. 1185–1200, Jul. 2010.

[11] S. D. Blunt, J. G. Metcalf, C. R. Biggs, and E. Perrins, "Performance characteristics and metrics for intra-pulse radar-embedded communications," *IEEE J. Sel. Areas Commun.*, vol. 29, no. 10, pp. 2057–2066, Dec. 2011.

[12] R. M. Mealey, "A method for calculating error probabilities in a radar communication system," *IEEE Trans. Space Electron. Telemetry*, vol. 9, no. 2, pp. 37–42, Jun. 1963.

[13] S. D. Blunt, M. R. Cook, and J. Stiles, "Embedding information into radar emissions via waveform implementation," in *Proc. Int. Waveform Divers. Design Conf.*, Niagara Falls, Canada, Aug. 2010, pp. 8–13.

[14] J. Euziere, R. Guinvarc'h, M. Lesturgie, B. Uguen, and R. Gillard, "Dual function radar communication time-modulated array," presented at the Int. Radar Conf., Lille, France, Oct. 2014.

[15] C. Alabaster, *Pulse Doppler Radar: Principles, Technology, Applications*. Edison, NJ, USA: SciTech Publishing, 2012.

[16] N. Levanon, "Mitigating range ambiguity in high PRF radar using inter-pulse binary coding," *IEEE Trans. Aerosp. Electron. Syst.*, vol. 45, no. 2, pp. 687–697, Apr. 2009.

[17] H. Meikle, *Modern Radar Systems*. Norwood, MA, USA: Artech House, 2008.

[18] X. Song, S. Zhou, and P. Willett, "Reducing the waveform cross correlation of MIMO radar with space time coding," *IEEE Trans. Signal Process.*, vol. 58, no. 8, pp. 4213–4224, Aug. 2010.

[19] J. Jakabosky, S. D. Blunt, and B. Himed, "Waveform design and receive processing for nonrecurrent nonlinear FMCW radar," in *Proc. IEEE Int. Radar Conf. (RadarCon 2015)*, Arlington, VA, USA, May 2015, pp. 1376–1381.

[20] L. Lo Monte, B. Himed, T. Corigliano, and C. J. Baker, "Performance analysis of time division and code division waveforms in co-located MIMO," in *Proc. IEEE Int. Radar Conf. (RadarCon 2015)*, Arlington, VA, USA, May 2015, pp. 794–798.

[21] Y. Li, S. A. Vorobyov, and V. Koivunen, "Ambiguity function of the transmit beamspace-based MIMO radar," *IEEE Trans. Signal Process.*, vol. 63, no. 17, pp. 4445–4457, Sep. 2015.

[22] S. Boyd and L. Vandenberghe, *Convex Optimization*. Cambridge, U.K.: Cambridge Univ. Press, 2009.

[23] I. Bekkerman and J. Tabrikian, "Target detection and localization using MIMO radars and sonars," *IEEE Trans. Signal Process.*, vol. 54, no. 10, pp. 3873–3883, Oct. 2006.

[24] L. Xu, J. Li, and P. Stoica, "Target detection and parameter estimation for MIMO radar systems," *IEEE Trans. Aerosp. Electron. Syst.*, vol. 44, no. 3, pp. 927–939, Jul. 2008.

[25] J. Li and P. Stoica, *MIMO Radar Signal Processing*. Hoboken, NJ, USA: Wiley, 2009.

[26] A. Hassanien and S. A. Vorobyov, "Why the phased-MIMO radar outperforms the phased-array and MIMO radars," in *Proc. 18th Eur. Signal Process. Conf.*, Aalborg, Denmark, Aug. 2010, pp. 1234–1238.

[27] A. Hassanien and S. A. Vorobyov, "Transmit energy focusing for DOA estimation in MIMO radar with colocated antennas," *IEEE Trans. Signal Process.*, vol. 59, no. 6, pp. 2669–2682, June 2011.

[28] Y. D. Zhang, M. G. Amin, and B. Himed, "Joint DOD/DOA estimation in MIMO radar exploiting time-frequency signal representations," *EURASIP J. Adv. Signal Process.*, vol. 2012, no. 102, pp. 1–10, Jul. 2012.

[29] A. Hassanien, M. G. Amin, Y. D. Zhang, and F. Ahmad, "Capon-based single snapshot DOA estimation in monostatic MIMO Radar," presented at the Symp. SPIE Sens. Technol. + Appl., Baltimore, MD, USA, Apr. 2015.

[30] A. Hassanien, M. G. Amin, Y. D. Zhang, and F. Ahmad, "High-resolution single-snapshot DOA estimation in MIMO radar with colocated antennas," in *Proc. IEEE Int. Radar Conf. (RadarCon 2015)*, Arlington, VA, USA, May 2015, pp. 1134–1138.

[31] A. Hassanien, S. A. Vorobyov, and A. Khabbazibasmenj, "Transmit radiation pattern invariance in MIMO radar with application to DOA estimation," *IEEE Signal Process. Lett.*, vol. 22, no. 10, pp. 1609–1613, 2015.

[32] H. L. Van Trees, *Optimum Array Processing*. New York, NY, USA: Wiley, 2002.

Aboulnasr Hassanien (M'08) received the Ph.D. degree in electrical and computer engineering from McMaster University, Hamilton, ON, Canada, in 2006. In 2006, he was a Research Associate with the Institute of Telecommunications, Darmstadt University of Technology, Germany. From 2006 to 2007, he was an Assistant Professor with the Department of Electrical Engineering, South Valley University, Aswan, Egypt. From 2008 to 2013, he was a Senior Research Associate with the Department of Electrical and Computer Engineering, University of Alberta, Edmonton, Alberta, Canada. Since 2014, he has been with Villanova University, Villanova, PA, where he is currently a Research Assistant Professor with the Center for Advanced Communications in the College of Engineering, and is the Director of the Wireless Communications and Positioning Laboratory.

Dr. Hassanien is a guest editor of the *International Journal of Antennas and Propagation* 2016 Special Issue on MIMO Antennas in Radar Applications. His research interests are in the general fields of signal processing and communications, with current activities focused on shared spectrum access, dual-function radar-communications, automotive signal processing, array signal processing, statistical signal processing, MIMO radar, space-time adaptive processing, detection and estimation, engineering optimization, and applications of signal processing in applied seismology.

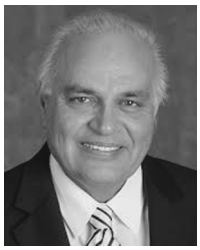

Moeness G. Amin (S'82–M'83–SM'91–F'01) received his Ph.D. degree from the University of Colorado, Boulder in 1984. He joined the Department of Electrical and Computer Engineering, Villanova University, in 1985 where he is now the Director of the Center for Advanced Communications. He is a Fellow of the International Society of Optical Engineering; Fellow of the Institute of Engineering and Technology; and Fellow of the European Association for Signal Processing. Dr. Amin is a Recipient of the 2014 IEEE Signal Processing Society Technical Achievement Award; Recipient of the 2009 Individual Technical Achievement Award from the European Association for Signal Processing; Recipient of the IEEE Warren D White Award for Excellence in Radar Engineering; Recipient of the IEEE Third Millennium Medal; Recipient of the 2010 NATO Scientific Achievement Award; Recipient of the 2010 Chief of Naval Research Challenge Award; Recipient of Villanova University Outstanding Faculty Research Award, 1997; and the Recipient of the IEEE Philadelphia Section Award, 1997. He was a Distinguished Lecturer of the IEEE Signal Processing Society, 2003–2004, and is currently the Chair of the Electrical Cluster of the Franklin Institute Committee on Science and the Arts. Dr. Amin has over 700 journal and conference publications in signal processing theory and applications. He co-authored 18 book chapters and is the Editor of the two books *Through the Wall Radar Imaging* and *Compressive Sensing for Urban Radar*, published by CRC Press in 2011 and 2014, respectively.

Yimin D. Zhang (SM'01) received his Ph.D. degree from the University of Tsukuba, Tsukuba, Japan, in 1988. He joined the faculty of the Department of Radio Engineering, Southeast University, Nanjing, China, in 1988. He served as a Director and Technical Manager at the Oriental Science Laboratory, Yokohama, Japan, from 1989 to 1995, a Senior Technical Manager at the Communication Laboratory Japan, Kawasaki, Japan, from 1995 to 1997, and a Visiting Researcher at the ATR Adaptive Communications Research Laboratories, Kyoto, Japan, from 1997 to 1998. He was with the Villanova University, Villanova, PA, from 1998 to 2015, where he was a Research Professor with the Center for Advanced Communications. Since 2015, he has been with the Department of Electrical and Computer Engineering, College of Engineering, Temple University, Philadelphia, PA, where he is currently an Associate Professor. His general research interests lie in the areas of statistical signal and array processing applied for radar, communications, and navigation, including compressive sensing, convex optimization, time-frequency analysis, MIMO system, radar imaging, target localization and tracking, wireless networks, and jammer suppression. He has published more than 270 journal articles and conference papers and 11 book chapters.

Dr. Zhang is an Associate Editor for the IEEE TRANSACTIONS ON SIGNAL PROCESSING, and serves on the Editorial Board of the *Signal Processing* journal. He was an Associate Editor for the IEEE SIGNAL PROCESSING LETTERS during 2006–2010, and an Associate Editor for the *Journal of the Franklin Institute* during 2007–2013. He is a member of the Sensor Array and Multichannel Technical Committee of the IEEE Signal Processing Society.

Fauzia Ahmad (S'97–M'97–SM'06) received her Ph.D. degree in electrical engineering from the University of Pennsylvania, Philadelphia, PA, in 1997. Since 2002, she has been with the Villanova University, Villanova, PA, where she is currently a Research Professor with the Center for Advanced Communications in the College of Engineering, and is the Director of the Radar Imaging Laboratory. She is a Senior Member of the Institute of Electrical and Electronics Engineers (IEEE), 2006 and a Senior Member of the International Society for Optics and Photonics (SPIE), 2012. Her general research interests are in the areas of statistical signal and array processing, radar imaging, radar signal processing, compressive sensing, waveform diversity and design, target localization and tracking, direction finding, and ultrasound imaging. She has published more than 190 journal articles and peer-reviewed conference papers and six book chapters in the aforementioned areas.

Dr. Ahmad is an Associate Editor of the IEEE TRANSACTIONS ON SIGNAL PROCESSING and IEEE GEOSCIENCE AND REMOTE SENSING LETTERS. She also serves on the Editorial Boards of the *IET Radar, Sonar & Navigation* and the SPIE/IS&T *Journal of Electronic Imaging*. She is a member of the Sensor Array and Multichannel Technical Committee of the IEEE Signal Processing Society and a member of the Radar Systems Panel of the IEEE Aerospace and Electronic Systems Society. She also chairs the SPIE Conference Series on Compressive Sensing. Dr. Ahmad is the Lead Guest Editor of IEEE SIGNAL PROCESSING MAGAZINE March 2016 Special Issue on Signal Processing for Assisted Living. She was the Lead Guest Editor of the SPIE/IS&T *Journal of Electronic Imaging* April–June 2013 Special Section on Compressive Sensing for Imaging and the Lead Guest Editor of the *IET Radar, Sonar & Navigation* February 2015 Special Issue on Radar Applied to Remote Patient Monitoring and Eldercare.